Chapter IX

Summary & Conclusion

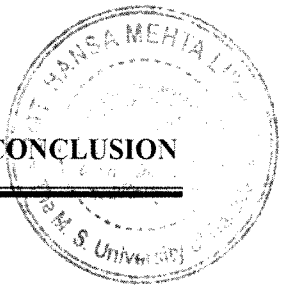

Since time immemorial, man has been on look out for new inventions, as a step towards better living. Many discoveries or inventions have found new usage in addition to their existing role. For many diseases, a substantial number of therapeutically effective compounds already exist but have not found the desired use due to biopharmaceutical limitations. Diabetes mellitus (DM) is one of the most common non-communicable diseases globally and Type II diabetes (T2DM) accounts for about 90 to 95% of total diabetics. Alzheimer's disease, the most common cause of dementia in elderly humans, occurs when neurons in the memory and cognition regions of the brain are accompanied by massive accumulation of abnormal fibrous amyloid β-protein (Aβ) at intracellular and extracellular sites, together with widespread neuronal cell loss. Preliminary results of clinical studies consistently suggested that restoring adequate levels of insulin and glucose by using a thiazolidinedione, facilitates memory in patients with Alzheimer's disease. This evidence has led to the notion of metabolic insufficiency or gluco-regulatory impairment in Alzheimer's disease and has provided a strong rationale for the therapeutic use of drugs, such as thiazolidinediones, that increase insulin sensitivity and glucose consumption.

The main obstacle in the treatment neuronal diseases is the presence of blood brain barrier (BBB), which selectively regulates and limits the amount and types of therapeutic agents permeating into the brain parenchyma. It is the lining of the brain capillary endothelial cells (BCEC), which forms the tight junctions and express efflux transport properties of the BBB that restrict and control the exchange of nutrients or bioactive substances between the peripheral

bloodstream and the central nervous system (CNS). This barrier acts as a unit to protect the brain from exogenous materials which could potentially damage the brain tissues.

One way of achieving the highest concentration of drug in the brain is to inject the drug intra-ventricularly in the brain. The second way used was to target the drug to cross BBB after intra-venous injection. Nearly all the drugs, particularly neuropharmaceuticals, cannot cross the BBB. Only drugs which are highly lipophilic or small enough in size usually enter the brain. To solve the problem of drug delivery across the BBB, the conventional invasive strategies such as intraventricular or intracerebral (transcranial) delivery and temporary impairment of the BBB are no longer feasible in consideration of the cost-benefit ratio for patients. They are often associated with high risk of infection, limited delivery area, drug diffusive resistance from interstitial fluid, high pre- and post-surgical cost or even serious clinical side effects in the case of high-dose therapy. Therefore, non-invasive approaches are imminent to be discovered and developed in view of the advantages of manipulating endogenous transport systems to overcome the BBB without physically interfering with the brain tissues which otherwise may cause medical complications. Various strategies like enhancing the lipophilicity of the drugs, use of prodrugs, disruption of the BBB, carrier and receptor mediated drug delivery, colloidal drug delivery, alternative route of administration through the intranasal route have been explored for enhancing the drug delivery to brain. Amongst the various strategies proposed for improving drug delivery to brain, the research on exploitation of nanoparticles as vectors is gaining great impetus. Nanoparticles alter the characteristics and tissue distribution pattern of drug and allow the passage of

inaccessible drugs to the brain. Nanoparticles of biodegradable polymers are safe and also provide prolonged release of the drug.

Our interest was in investigating the biodegradable nanoparticles (NPs) as a drug delivery system for neuroprotective agents. The intra-venous injection of the drug loaded nanoparticles is expected to enhance the retention of the drug in the brain for prolonged period of time compared to the drug solution which does not cross the BBB. The advantage of these NPs is their sustained release property, and since the drug is entrapped, it is not exposed to the BBB endothelial membrane associated efflux transporters and thus can result in greater cellular drug uptake than that from drug in solution. Further, the slow intracellular release of drug from the NPs localized inside the cells is expected to sustain the drug effect, and hence can increase its overall therapeutic efficacy. It is also important that the formulation should be non toxic to the brain. So biodegradable and biocompatible polymer i.e. PLGA was used for preparation of the nanoparticles.

Targeted drug delivery is one of the approaches receiving considerable attention in the recent years. The ideal requirement of targeted drug delivery system is that the distribution to the other organs is reduced and high concentration of the drug is maintained at the diseased site for prolonged period of time.

Almost in all circumstances, essential nutrients such as glucose, amino acids and vitamins for proper brain functioning are required and the general route of absorbing these nutrients is through the BBB. As a result, specific receptors (biomarkers) on the BBB responsible for transporting the nutrients are crucial in governing the nutrients entry to and from the brain tissues. The BBB is provided with active transport mechanisms like carrier mediated transport,

adsorption mediated transport and receptor mediated transport for nutrients supply to the brain.

Receptor mediated transport (RMT) employs the interaction of ligand with the receptors located at the luminal membrane, for the transport of nutrients across the BBB. Receptors localized at the BBB include the transferrin receptor, the insulin receptor, and the transporters for low-density lipoprotein, lectin and insulin-like growth factors. Of various categories in endogenous transport systems, receptor-mediated transport is an attractive strategy due to a few reasons such as circumvention of the multi-drug resistant (MDR) P-glycoprotein (Pgp) efflux transporter in the BBB and cancer cells, high specificity in ligand-receptor binding, low immunological response, no restriction of cargo size and the ability to transport macromolecules such as proteins and peptides across BBB. It is these endogenous transport systems that serve as the platform for developing new drug formulations that can reach to the brain by exploiting these highly selective molecular carriers.

Transferrin receptor, a transmembrane glycoprotein, over-expressed on the BBB at the luminal side facilitates the delivery of iron to the brain through endocytosis of the iron binding protein transferrin. This receptor mediated transport mechanism can be useful for delivery of therapeutics to the brain. Surface engineering of the drug loaded polymeric nanoparticles by conjugation with transferrin alter the biodistribution characteristics of drug allowing its delivery across the BBB. This receptor is also over-expressed in many types of malignant tumors as well as in human tissues of liver, intestinal epithelium and erythroblasts, but the level of expression is nearly undetectable in other normal, non-dividing healthy tissues. Therefore, transferrin (Tf) has been widely studied and shown to be a promising molecular probe for targeted drug delivery to the

brain. As a result, various drug carriers employing Tf as a trojan to gain selective access to the CNS have been reported. Some examples of drugs delivered by this pathway include paclitaxel and daunorubicin as cancer therapeutic agents, quinine dihydrochloride and artemisinin as anti-malarial medications.

Alternatively, intranasal route also delivers the drug rapidly and directly to brain by circumventing the BBB. The intranasal route has several advantages like non-invasive route of delivery, transport of the drug directly to brain with reduction in drug delivery to the non target sites, reduction in the dosing and the associated side effects. Administration of nanoparticles through intranasal route may not require any ligand attachment or any surface modifier for delivery to brain.

Drugs such as Pioglitazone and Rosiglitazone have proved efficacy in controlling Alzheimer's disease in clinical setting but they are ineffective when administered through oral route due to their inability to penetrate BBB. Pioglitazone and Rosiglitazone have been reported to be substrate for Pgp and MDR efflux transporters and are effluxed at BBB and hence inadequately available in brain. Hence it was thought worthwhile to develop targeted nanoparticulate system in an attempt to target the drug delivery system to the brain and release the drug in brain to have a simultaneous anti-diabetic and anti-alzheimer's activity.

Hence, development of nanoparticulate carrier of biodegradable polymers (such as PLGA) in combination with transferrin as a brain-targeting ligand for treatment of the Alzheimer's disease in conjunction with effective diabetes management is the backbone of this study. Firstly, the nanoparticulate formulations encapsulating Pioglitazone/Rosiglitazone with Tf surface conjugation were fabricated. Secondly, the characteristics of the actively targeted

nanoparticles were compared with non-targeting nanoparticles with regard to particle size, entrapment efficiency, surface morphology and *in vitro* drug release. Thirdly, the ex vivo cytoprotective activity was carried out using neuro-2a cell line to determine the targeting ability of transferrin-conjugated PLGA nanoparticles and to access the cytoprotective activity of developed formulations. Finally biodistribution study especially that in the brain and blood, of the transferrin-conjugated PLGA nanoparticles versus the non-targeting nanoparticles was studied in mice model.

It was hypothesized that incorporation of drug in the nanoparticles will alter the pharmacokinetics of drug making it long circulating and due to the presence of surface attached transferrin lead to targeted and enhanced delivery to the brain after intravenous administration of such nanoparticulate formulation. The efforts were also made to deliver the drug solution through intranasal route, for direct delivery to the brain by circumventing the blood brain barrier and for the cure of brain disorders or at least supplementary to parentral therapy.

Drug estimation in the nanoparticles and *in vitro* release medium was performed by UV spectrophotometry. The calibration curve of Pioglitazone HCl was prepared by UV spectrophotometry at 268 nm in solvent system of methanol : acetonitrile in ratio of 1:1. The linearity of Pioglitazone HCl was found to be 10-28 µg/ml (R^2=0.99). The recovery study for accuracy and precision was carried out at 20 µg/ml and the recovery was found to be more than 99%, indicating the reliability of the method.

The calibration curve of Pioglitazone HCl was also prepared by UV spectrophotometry in solvent system of methanol : acetonitrile : PBS (pH 7.4) : 0.1N Sodium Hydroxide solution in ratio of 1:1:1:7. The linearity of Pioglitazone

HCl was found to be 5-50 µg/ml (R^2=0.99). The recovery study for accuracy and precision was carried out at 25 µg/ml and found to be more than 99%, indicating the reliability of the method. The first standard curve was used in determination of drug entrapment in the nanoparticles whereas the later was used in determining the drug released from drug delivery system.

The standard curve of Rosiglitazone maleate was made at λ_{max} 246.8nm in methanol and the linearity of was found in the concentration range of 2-20 µg/mL (R^2=0.998). The recovery study for accuracy and precision was carried out at 10 µg/ml and was found to be more than 99%, indicating the reliability of the method. Similarly, standard curve of Rosiglitazone base was prepared at λ_{max} 246.2 in solvent system of acetonitrile : PBS (pH 7.4) (2:3) in the concentration range of 2-20 µg/mL. The regression coefficient of 0.9991 was obtained which confirmed an excellent linearity between concentration and absorbance. The recovery studies for accuracy and precision was carried out at 10 µg/ml and the recovery was found to be more than 99%.

Drug loaded nanoparticles were prepared by nanoprecipitation and emulsion solvent evaporation technique. In nanoprecipitation technique, the basic process parameters like rate of addition of organic phase, stirring speed, volume of aqueous phase and stirring time were standardized before proceeding for the optimization of the formulation variables. The critical formulation parameters investigated included polymer concentration, loading drug, surfactant (Tween 80) concentration, stabilizer (PVA) concentration and volume of organic phase for polymer as well as for drug.

With the increase in entrapment efficiency, an increase in size and zeta potential was observed. However, PDI was found to decrease. The increase in size may be attributed to the entrapment of drug in the nanoparticles. The

entrapment efficiency of nanoparticulate formulation's increased with the increasing polymer concentration. High concentration of polymer in the internal phase could have increased the viscosity of the solution thus retarding diffusion in effect within or through the polymeric intermediate. The effect of initial drug loading on particle size and entrapment efficiency were investigated by varying the drug loading from 1 to 4 mg in 10 ml aqueous phase. Initial drug loading in the nanoparticulate formulations was optimized by keeping the PLGA concentration constant at 0.2% w/v. There was an increase in encapsulation efficiency with increase in drug loading from 1 mg to 2 mg but it decreased at 3 mg and at further increase, i.e. at 4 mg loading, nanoparticles were not formed as drug got precipitated out form the aqueous phase during solvent evaporation phase. The surfactant at fixed concentration can solubilize a particular amount of drug in the aqueous phase, above which the excess drug precipitates out.

Tween-80 was added in the aqueous phase to improve the wetting of drugs, pioglitazone and rosiglitazone. It was observed that at least 0.001% tween-80 was required to obtain a uniform dispersion. Further, the particle size got reduced upon increasing Tween-80 and decrease in particle size may be due to the increasing surfactant action of Tween-80 with its increasing concentration which solubilized the drug more and hence decreased the entrapment. PVA in four different concentrations (0.25, 0.5, 0.75, and 1.0% w/v of the aqueous phase) was used to optimize the stabilizer concentration required to obtain a stable particulate preparation. A stabilizer is required for nanoparticulate systems to prevent coalescence and formation of agglomerates during and after the emulsification process. The stabilizer concentration with PVA was optimized at 0.25% w/v because, at higher concentration, reproducibility was compromised and also did not give any significant advantage in terms of particle size and

entrapment efficiency. Increasing PVA concentration resulted in increased particle size and also zeta potential where as PDI decreased. The particle size and drug entrapment efficiency were found to be inversely proportional to the organic : aqueous phase ratio. As the organic : aqueous phase ratio was increased, the particle size and drug entrapment efficiency decreased. Increase in the organic phase ratio leads to increased evaporation time causing slower polymer precipitation, due to the increased microenvironment provided by organic phase after dispersing in the aqueous phase, and there by formation of small particles.

After optimization of formulation variables, the process variables were optimized. In order to obtain particles of specific size and surface area, the effect of stirring speed was varied from 250 to 550 rpm. An increase in the stirring speed from 250 rpm to 450 rpm leads to a decrease in the particle. On further increasing the stirring speed to 550 rpm there was no significant decrease in the particle size. Four stirring times were used in the preparation of nanoparticles in order to study the effect of evaporation of organic phase on the characteristics of the nanoparticles. It was found that increase in stirring time from 3 hrs to 5 hrs led to a decrease in the particle size. Further increase in the stirring time up to 6 hrs led to agglomeration of the nanoparticles. Thus, 5 hrs was chosen as an optimum stirring time.

In emulsion solvent evaporation technique, the basic process parameters like rate of addition of organic phase, stirring speed, volume of aqueous phase, stirring time and sonication parameters like sonication cycle, amplitude and time of sonication were standardized before proceeding for the optimization of the formulation variables. The formulation PIO-NPE2 and ROS-NPE2 where 0.2% w/v PLGA concentration was used as principle polymer exhibited homogenous

size distribution and was selected and used for further studies. Loading drug amount was optimized in the formulations by the keeping concentration of PLGA constant (0.2% w/v). The loading amount was varied from 1 - 4 mg. The observations suggested that formulations PIO-NPE6 and ROS-NPE6 prepared by using 2 mg of drug (Pioglitazone or Rosiglitazone) exhibited homogenous size distribution and maximum entrapment efficiency which were considered to be optimum. To optimize the concentration of Tween-20 in the formulations, formulations PIO-NPE11 and ROS-NPE11 prepared by using 0.005% w/v of Tween-20 exhibited minimum particle size with maximum drug entrapment and thus 0.005% w/v of Tween-20 was selected as optimum surfactant concentration.

Formulations were subsequently optimized for stabilizer (polyvinyl alcohol) concentration (0 - 0.2% w/v). PVA acts as a stabilizer by preventing aggregation of nanoparticles and also enhance entrapment efficiency and decrease PDI. The results indicate that formulations PIO-NPE15 and ROS-NPE15 prepared by using 0.1% of PVA exhibited optimum particle size with reasonable drug entrapment. It has previously been reported that use of PLX as stabilizer decreases particle size but compromises entrapment efficiency. Polaxamer acts as stabilizer which prevents the particle aggregation and helps to stabilize the newly generated surfaces. Thus the formulations PIO-NPE18 and ROS-NPE18 where 0.1 %w/v Polaxamer concentration was used as stabilizer exhibited narrow particle size distribution and was selected for further studies No statistically significant correlation was found between particle size and drug entrapment efficiency when organic : aqueous phase ratio was increased. In PIO formulations, as the organic : aqueous phase ratio of polymer was increased, the particle size decreased whereas drug entrapment efficiency initially increased and then decreased. In ROS formulations, as the organic : aqueous phase ratio of

polymer was increased, correlation was found between particle size or drug entrapment efficiency. In order to obtain particles of large surface area, the effect of sonication time (1 to 4 min) was studied. A significant effect of sonication time was observed on the formation of nanoparticles as low emulsification time led to precipitation of polymer whereas high emulsification time caused decrease in entrapment efficiency. The sonication of 3.5 min for PIO and 3 min for ROS formulations was found to produce optimum sized nanoparticulate formulations with a uniform size distribution and maximum entrapment efficiency.

The effect of stirring speed (250 to 550 rpm) was observed for the nanoparticulate formulations. The stirring speed of 450 rpm was found to produce formulations of narrow size distribution, maximum entrapment efficiency and thus 450 rpm as stirring speed was used in formulations.

The results clearly indicate that although particles obtained by emulsion solvent evaporation technique were of larger size as compared to nanoprecipitation technique, but significantly higher entrapment efficiency was obtained with emulsion solvent evaporation technique. Thus the later technique was selected for nanoparticle preparation and the particles so formed were processed to ligand conjugation and subsequent studies.

Optimized batch of Pioglitazone nanoparticles (PIO-NP) and Rosiglitazone nanoparticles (ROS-NP) were conjugated with transferrin by formation of amide linkage between carboxylic acid group of PLGA and amine functionalities of transferrin. Drug (Pioglitazone/Rosiglitazone) loaded PLGA nanoparticles were suspended in PBS (pH 5.0) and activated by addition of 1-ethyl-3-(3-dimethyl amino propyl) carbodiimide (EDAC). The suspension was stirred continuously for 0.5 h below 15^{0}C and protected from light. Subsequently, N-Hydroxy succinimide (NHS) was added and the stirring was continued for

another 0.5 h while maintaining the temperature below 15°C. Finally the suspension of activated nanoparticles in PBS (pH 5.0) was incubated with transferrin and stirred for another 1.0 h while maintaining the temperature below 15°C. Transferrin conjugated nanoparticles were then collected by centrifugation at 11,000 rpm for 15 min at 2°C and washed five times with PBS (pH 7.4) for the removal of uncoupled transferrin.

FTIR study was performed in order to confirm the coupling of transferrin to PLGA nanoparticles. In case of transferrin anchored pioglitazone nanoparticles (Tf-PIO-NP), the presence of a characteristic sharp peak near 3282.65 cm^{-1} indicated -N-H stretching which indicates the presence of amine group on the surface of PLGA nanoparticles. The peak near 1548.11 cm^{-1} corresponds to the N-H bending vibrations for amide II and peak near 1645.45 cm^{-1} corresponding to the stretching amide I for −C=O group indicates the presence of −C=O of amide group. This confirmed the formation of amide bond (-CO-NH) between ligand and PLGA nanoparticles.

Similarly in case of transferrin anchored rosiglitazone nanoparticles (Tf-ROS-NP), the presence of a characteristic sharp peak near 3281.10 cm^{-1} indicated -N-H stretching which indicates the presence of amine group on the surface of PLGA nanoparticles. The peak near 1548.35 cm^{-1} corresponds to the N-H bending vibrations for amide II and peak near 1646.48 cm^{-1} corresponding to the stretching amide I for −C=O group indicates the presence of −C=O of amide group. This confirmed the formation of amide bond (-CO-NH) between ligand and PLGA nanoparticles.

The particle size of optimized PIO-NP and Tf-PIO-NP was 225.8±10 nm and 394±7 nm respectively. Their PDI were 0.332 and 0.438 respectively. Further the particle size of ROS-NP and Tf-ROS-NP was found to be 235.9±6 nm and

389±8 nm respectively and their PDI was 0.268 and 0.412 respectively. This shows the homogeneity in particle size.

The drug content of pioglitazone entrapped in PIO-NP and Tf-PIO-NP was found to 41.3±1.3 and 29.3±1.0 % respectively. Similarly, the drug content of rosiglitazone entrapped in ROS-NP and Tf-ROS-NP was found to be 39.4±1.4 and 29.2±1.1 %, respectively. Further, the content of pioglitazone and rosiglitazone in their nasal solutions was found to be 99.7±1.5 and 99.8±1.2 % respectively.

The measurement of zeta potential by Malvern Zetasizer revealed that PIO-NP and ROS-NP exhibited a negative zeta potential of -11.2 and -12.3 mV. The negative value of zeta potential may be attributed to negatively charged carboxylic groups ($-COO^-$) tailored at the surface of the PLGA. Further, the value of zeta potential augmented to -4.8 and -2.1 mV in case of Tf-PIO-NP and Tf-ROS-NP. This increase in zeta potential may be ascribed to conjugation of carboxylic groups with amine functionalities (NH_2) upon binding of Transferrin to unconjugated nanoparticles.

The TEM photographs reveal nanoparticles to be spherical and nanometric in size. The results also indicate an increase in size of PLGA nanopaticle upon conjugation of Transferrin as a ligand.

Physicochemical interactions if any, occurred between drug & excipients during formulation was checked by XRD and TGA.

TGA is a very useful technique for the investigation of thermal properties of nanoparticles, providing both qualitative and quantitative information about the presence of drug inside the nanoparticles. The peaks observed at temperature above 250°C might be degradation exotherm of Pioglitazone, Rosiglitazone, PLGA polymer, Tf-PIO-NP, Tf-ROS-NP. The decrease in weight obtained in TGA of Pioglitazone, Rosiglitazone and PLGA at 188.4°C, 155.0°C and 50.5°C

represents the melting of Pioglitazone, Rosiglitazone and PLGA. In case of TGA of Tf-NP-PIO nanoparticulate formulation, the decrease in weight was obtained at 60.2°C and 195.6°C and this confirms presence of PLGA and Pioglitazone in the nanoparticulate formulation respectively. Similarly, TGA of Tf-NP-ROS formulation, the decrease in weight was obtained at 154.8°C. The study thus confirms presence of PLGA and Rosiglitazone in the nanoparticulate formulation and also absence of any type of physicochemical interaction of the drug with PLGA.

X-ray diffractograms reveal information on the crystal structure of different polymorphs and pseudopolymorphs. PLGA exhibits no characteristic crystalline peaks and confirmed its amorphous nature. The XRD patterns of Pioglitazone and Rosiglitazone showed typical sharp peaks of drug crystals. X-Ray diffraction of physical mixture of Pioglitazone and PLGA was obtained. On comparison of XRD of physical mixture with PLGA and Pioglitazone, the XRD of physical mixture clearly indicates characteristic crystalline peaks of drug and amorphous nature of PLGA.

Further, In case of XRD of PIO-NP and Tf-PIO-NP, the specific drug crystal peaks were not observed. It may be thought that free drug crystallites and exhibit sharp specific crystal peaks when existed as drug crystals but the same drug when existed as molecular dispersion inside the nanoparticles exhibited no sharp peaks after entrapment into it. Hence possibly the drug gets dissolved during the formation of nanoparticles and subsequently gets entrapped as amorphous form.

Similar results were observed in case of Rosiglitazone loaded unconjugated and Transferrin anchored PLGA nanoparticles'

The *in vitro* release study was performed using the dialysis tube diffusion method. An initial burst release for 4 hrs was obtained. The % cumulative drug release of 18.56 and 13.18 % was obtained from PIO-NP and Tf-PIO-NP, respectively at the end of 4 hrs. This burst release may be attributed to immediate dissolution of surface adsorbed drug or the drug release from the outermost layer of the nanoparticles. Subsequently sustained release pattern was obtained for 13 days with a cumulative release of 95.3, 81.4, 96.27 and 82.51 % from PIO-NP, Tf-PIO-NP, ROS-NP and Tf-ROS-NP respectively. These results may be attributed to hydrophobic nature of drug that was entrapped by hydrophobic interaction of hydrophobic polymer of the polymeric nanoparticles. The results also indicate a decrease in drug release upon transferrin conjugation. This may be attributed to production of additional barrier to drug diffusion upon ligand conjugation.

The stability studies of optimized formulations were carried out to assess the effect of different storage conditions on the integrity of prepared drug delivery systems. The stability study of nanoparticulate formulations was carried out after storing them at 5°C ± 2°C and 25°C ± 2°C at 60 ± 5% RH for upto 6 months. The particle size and PDI were not substantially affected in formulations when stored at 5°C ± 2°C for 6 months. However, the average particle size and PDI were found to increase significantly when formulations were stored at 25°C ± 2°C at 60 ± 5% RH. The increase in particle size was more prominent after 4 months of storage and still more prominent after 6 months storage as compared to storage for 2 months and this might be due to aggregation of nanoparticles. The nanoparticles might have aggregated due to absorption of moisture by nanoparticles resulting in coalescence of nanoparticles to form larger particles.

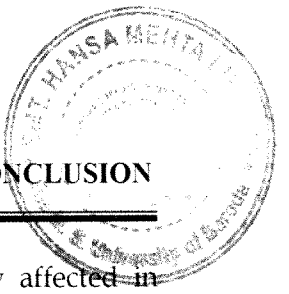

After 6 months storage period, zeta potential was slightly affected in formulations stored at 5°C ± 2°C. When formulations were stored at 25°C ± 2°C at 60 ± 5% RH, the zeta potential of the nanoparticles shifted towards the zero value for both Tf conjugated and unconjugated nanoparticles. This might be due to the acidic condition produced by the degradation of PLGA into lactic and glycolic acid moieties.

The formulations were found to be stable during 6 months stability studies when stored at 5°C ± 2°C. However at 25°C ± 2°C, drug content was decreased and maximum decrease in percent residual drug content was found for formulations stored for 6 months. More than 95% drug was retained for 6 months in all the nanoparticles when stored at 5°C ± 2°C, while less than 95% drug was found to be retained in unconjugated nanoparticles after 6 months when stored at 25°C ± 2°C. This could be due to the moisture absorbed by the nanoparticles at higher humidity and temperature possibly resulting in instability and degradation of PLGA leading to generation of acidic moieties which degraded entrapped drug and hence the nanoparticles showed a lesser drug content after storage period.

Transferrin conjugated and unconjugated nanoparticulate formulations of pioglitazone and rosiglitazone were found to be stable at 5°C ± 2°C when stored for 6 months and such formulations should be stored at refrigerated conditions (5°C ± 2°C) for better stability and efficacy.

The hemolytic toxicity study of PIO solution, ROS solution, blank PLGA NP, PIO-NP, ROS-NP, Tf-PIO-NP and Tf-ROS-NP was performed to assess the toxicity of drugs and their formulations to RBC's on i.v. administration of formulations. The hemolytic toxicity of PIO and ROS solution was found to be 4.2±0.8% and 5.1±0.9%, respectively. The hemolytic toxicity of blank PLGA NP's

was found to be 1.3±0.2% suggesting the better biocompatibility of the blank polymeric formulation and signifying the suitability of prepared formulation for the delivery of drugs which is also desired for an ideal drug delivery application. The PIO-NP and ROS-NP were found to have 2.4±0.4% and 2.6±0.5% hemolytic toxicity. Lowest haemo-toxicity was observed with Tf-PIO-NP (1.9±0.3%) and Tf-ROS-NP (2.1±0.2%) and this may be ascribed to the synergistic effect of entrapment of drug in the nanoparticles and a stearic double barrier provided by transferrin conjugation that further minimized the release of drug and its interaction with RBC's. It can be concluded from this study that transferrin anchored PLGA NP's are safer for use as an intravenous carrier of the drugs.

The *ex vivo* cytoprotective activity of the optimized nanocarrier systems against cytotoxic Aβ was assessed on mouse neuroblastoma (neuro-2a) cells. In the presence of Aβ, the cell viability was drastically reduced in the wells of control group (77.1±3.6%). When cells were incubated with Aβ along with PIO solution (in DMSO), PIO-NP and Tf-PIO-NP, at a concentration of 5.0μM/ml, the percent cell viability was found to be 67.7±2.3% (after subtraction of solvent toxicity), 85.8±3.7% and 86.8±3.4%, respectively. Similarly, in presence of Aβ, ROS solution (in PBS pH 7.4), ROS-NP and Tf-ROS-NP, at a concentration of 5.0μM/ml, showed percent viability of 81.7±3.0%, 107.2±2.8% and 138.5±2.1%, respectively after 48 h of incubation. The drug loaded nanoparticulate formulations have significantly decreased the cell death mediated by Aβ and this might be due to the cell protective action of drugs (PIO and ROS) against Aβ induced cell death. Nanoparticulate formulations, both unconjugated and transferrin conjugated nanoparticles, were found to have higher cytoprotective activity as compared to corresponding drug solutions as very high percent cell viability was observed. The higher cytoprotective activity of the Tf conjugated

nanoparticles was confirmed by microscopic examination of cells after incubation peroid. This may be attributed to the presence of transferrin on the NP's surface which possibly facilitated greater internalization of NP's and hence drug, via its receptors present on the surface of neuroblastoma cells. Augmented entry in the cells followed by sustained release of drug might be the rational for enhanced % cell survival.

The intracellular disposition characteristics of Tf-conjugated NPs following their cellular uptake via Tf receptors could have been different from that of unconjugated NPs via nonspecific endocytic pathway, thus influencing the NP uptake, their intracellular retention, and hence the therapeutic efficacy of the entrapped drug. The mechanism of greater proliferative activity of the drug with conjugated NPs was determined to be due to their greater cellular uptake and reduced exocytosis compared to that of unconjugated NPs, thus leading to higher and sustained intracellular drug levels.

The cytoprotective action was found to be dose dependent, as evident from the results that with increase in drug amount in formulations (0.5 μM to 5.0 μM), the cell viability increased, indicating an increase in the cytoprotective activity of the drug loaded nanoparticles at higher dose.

The prepared nanoparticulate carriers were further tested for targeting efficiency by gamma scintigraphy. $^{99m}TcO_4^-$ was used for the radiolabeling of nanoparticulate formulations as well as both drugs (Pioglitazone and Rosiglitazone) due to its easy availability, cost effectiveness and low radiation dose. Radiolabeling was optimized by taking three factors into consideration i.e. amount of stannous chloride dihydrate, pH of the incubation medium, and incubation time.

It was observed that addition of 200 μg of stannous chloride resulted in highest radio-labeling efficiency with minimum formation of radiocolloids or free ^{99m}Tc. At lower concentration of stannous chloride (<200μg/ml) the remaining activity was due to free ^{99m}Tc, whereas at higher concentration (>200μg/ml) radiocolloids were formed.

As the pH of incubation medium was increased from 5 to 7, the radio-labeling also increased from 79.51 to 98.83% for PIO-S, 82.49 to 98.14% for PIO-NP and 84.25 to 97.83% for Tf-PIO-NP nanoparticles. Further increase in the pH resulted in the reduction of radio-labeling efficiency. Similar effect of pH was also observed on radiolabeling of rosiglitazone and its nanoparticlulate formulations. The optimum incubation time required for maximum radiolabeling was found to be 30 min for all the formulations. Further increase in incubation time did not show any significant increase in the radiolabeling efficiency.

In the present study, the active targeting strategy utilizing the over-expression of transferrin receptors on Blood Brain Barrier was utilized where transferrin conjugated nanocarriers were targeted to brain with more efficiency. The biodistribution of radiolabeled pioglitazone, pioglitazone loaded nanoparticles, rosiglitazone and rosiglitazone loaded nanoparticles was studied in mouse model (swiss albino) for 6 h after single i.v./oral/nasal administration.

Upon, intranasal delivery, highest radioactivity was again recovered from liver and was 17.84±0.44 % and 17.29±0.72 % ID/g in case of PIO-S and ROS-S, respectively at the end of 6 hrs. Further, some radioactivity was also recovered from brain (0.22±0.02 % ID/g and 0.19±0.02 % ID/g with PIO-S and ROS-S, respectively) at the end of 6 hrs. This indicated the direct transport of nanoparticles to the brain through the olfactory route bypassing the blood brain

barrier (Illum, 2000). However, the amount of radioactivity recovered may not be considered to be high enough to be able to produce any remarkable therapeutic effect. When ROS-S was intravenously administered, the radioactivity recovered in the liver was 9.04±0.41 % ID/g. The results obtained may be attributed to liver being the major organ of metabolism of the drug(s).

Nanoparticles showed enhanced circulation time when compared with free drugs. Transferrin conjugated nanoparticles encapsulating pioglitazone showed greater localized radioactivity in brain as compared to intranasally administered drug solution. Furthermore, in case of PIO-NP, slightly increased radioactivity as compared to intranasal formulation was recovered from brain. The studies clearly indicated superiority of the transferrin conjugated nanoparticles over the free drugs and unconjugated nanoparticles in increasing the accumulation of PIO and ROS within the brain.

Transferrin conjugation of nanoparticles altered the biodistribution of drugs. The distribution of Tf-PIO-NP was found to be 2.23±0.31% in brain after 6 hrs post injection which was almost 10 and 3 times more as compared to PIO-S (nasal) and PIO-NP (i.v.) respectively. Similar results were also observed with Tf-ROS-NP. Thus ligand coupling to the nanoparticulate surface enhanced their delivery to the brain. The receptor mediated endocytosis may possibly be responsible for significantly enhanced uptake of transferrin conjugated nanoparticles in comparison to unconjugated NPs.

The order of radioactivity recovered in brain after 6 hrs of administration for various pioglitazone formulations was Tf-PIO-NP (i.v.) > PIO-NP (i.v.) > PIO-S (intranasal) > PIO-D (oral). The order of radioactivity recovered in brain after 6 h of administration of various rosiglitazone formulations was Tf-ROS-NP (i.v.) > ROS-NP (i.v.) > ROS-S (intranasal) > ROS-S (i.v.) > ROS-S (oral).

The distribution of rosiglitazone when administered as ROS-S was more in kidney in comparison to unconjugated and transferrin conjugated nanoparticles. At 0.5 hrs after intravenous injection, rosiglitazone showed higher accumulation in kidney at 4.30±0.21 %ID/g with respect to 1.32±0.08 %ID/g for ROS-NP and 1.54±0.14 %ID/g for Tf-ROS-NP, indicating fast clearance of drug solution than the nanoparticulate formulation. The radioactivity measured also indicated higher accumulation of unconjugated and conjugated nanoparticles than plain drugs in the lungs. This enhanced deposition might have resulted due to the size and particulate nature of the nanoparticles.

Based on the whole-body images, it could be concluded that organs of reticulo-endothelial system were responsible for a major uptake of the drug when administered as solution. Images at different time intervals after administration of nanoparticulate formulation and free drugs have been shown in scintigraphs. These images clearly illustrate the superiority of transferrin linked nanocarriers over uncoupled nanocarriers in drug targeting to the brain.

The plasma and tissue biodistribution studies have shown higher radioactivity recovery from brain with ligand coupled nanoparticles as compared to unconjugated nanoparticles and free drugs indicating the efficacy of carrier for brain targeting of the drugs. Therefore the results confirmed that the developed transferrin conjugated delivery systems possessed an enhanced brain targeting activity in mice and are capable of reducing systemic and hepatic toxicity induced by anti-diabetic drugs when administered for long term and these formulations may be potentially useful in the treatment of brain disorders.

Conclusion

- PLGA nanoparticles entrapping Pioglitazone and Rosiglitazone were successfully prepared using nanoprecipitation and emulsion solvent evaporation method.
- By careful optimization of different formulation and process variables; and characterizing them for size, size distribution, surface morphology, zeta potential and surface chemistry; drug entrapment efficiency and *in vitro* release profile, the nanoparticles with the desired nano size range, high % drug entrapment and sustained release profile were achieved which were conjugated with transferrin for brain targeting.
- Transferrin conjugation to the prepared nanoparticles was confirmed by the FTIR study while the XRD and TGA studies indicated absence of any physicochemical interaction between drug and the excipients.
- The optimized nanoparticulate formulations were found to be most stable at 5±2°C suggesting their storage in refrigerator.
- **The comparison of the cytoprotective activity in murine neuro-2a cells, in presence of β-amyloid, Tf-conjugated nanoparticles demonstrated significant % cell viability indicating cytoprotective activity or probably cell proliferative activity while unconjugated nanoparticles showed a very less cytoprotective activity. Thus transferrin conjugated nanoparticles entrapping pioglitazone & rosiglitazone protected neuro-2a cells in presence of β-amyloid responsible for Alzheimer's.**
- The results of *in-vivo* biodistribution studies carried out using swiss albino mice revealed that Tf-conjugated nanoparticulate formulations were able to preferentially localize within the brain. An important finding of this study was that the drug via conjugated as well as unconjugated nanoparticulate formulation's showed a reduced accumulation of drugs in the kidney which was highly desirable.

- Further the targeting efficiency tested by gamma scintigraphy indicated a finding that the intranasally administered drug solutions were transported directly to the brain through the olfactory route bypassing the blood brain barrier. However, the amount of radioactivity recovered may not be considered to be sufficient to be able to produce any remarkable therapeutic effect in comparison to i.v. administration of transferrin conjugated nanoparticles.

In conclusion, the design of actively targetable nanoparticles as drug carriers by coupling transferrin, could be one of the promising solutions to deliver drugs across BBB. Thus, the present study led to some interesting findings which may be utilized for improving the therapeutic efficacy of anti-diabetic drugs through exploitation of novel approach of receptor mediated targeted delivery of these drugs for the control of Alzheimer's disease.

Future Scope of study:

Further the studies may be warranted to establish safety and efficacy coupled with scale up and feasibility in order to establish applicability of the transferrin conjugated nanoparticles of thiazolidinediones such as Pioglitazone and Rosiglitazone for control of Alzheimer's.